Pediatric SARS, H1N1, MERS, EVALI, and Now Coronavirus Disease (COVID-19) Pneumonia: What Radiologists Need to Know

Alexandra M. Foust[1]
Abbey J. Winant[1]
Winnie C. Chu[2]
Karuna M. Das[3]
Grace S. Phillips[4]
Edward Y. Lee[1]

OBJECTIVE. The purpose of this article is to review new pediatric lung disorders—including disorders that have occurred in recent years years such as severe acute respiratory syndrome (SARS), swine-origin influenza A (H1N1), Middle East respiratory syndrome (MERS), e-cigarette or vaping product use–associated lung injury (EVALI), and coronavirus disease (COVID-19) pneumonia—to enhance understanding of the characteristic imaging findings.

CONCLUSION. Although the clinical symptoms of SARS, H1N1, MERS, EVALI, and COVID-19 pneumonia in pediatric patients may be nonspecific, some characteristic imaging findings have emerged or are currently emerging. It is essential for radiologists to have a clear understanding of the characteristic imaging appearances of these lung disorders in pediatric patients to ensure optimal patient care.

Keywords: coronavirus disease, COVID-19, e-cigarette or vaping product use–associated lung injury, EVALI, H1N1, MERS, Middle East respiratory syndrome, SARS, severe acute respiratory syndrome, swine-origin influenza A, viral pneumonia

doi.org/10.2214/AJR.20.23267

A. M. Foust and A. J. Winant contributed equally to this study.

Received April 1, 2020; accepted without revision April 2, 2020.

[1]Department of Radiology, Boston Children's Hospital, Harvard Medical School, 300 Longwood Ave, Boston, MA 02115. Address correspondence to A. M. Foust (Alexandra.Foust@childrens.harvard.edu).

[2]Department of Imaging and Interventional Radiology, The Chinese University of Hong Kong, Prince of Wales Hospital, Hong Kong, China.

[3]Department of Radiology, College of Medicine and Health Sciences, Al Ain, United Arab Emirates.

[4]Department of Radiology, Seattle Children's Hospital, University of Washington School of Medicine, Seattle, WA.

AJR 2020; 215:1–9

ISSN-L 0361–803X/20/2153–1

The early 21st century has seen the emergence of several severe outbreaks of pediatric lung illnesses such as contagious viral epidemics, including three coronaviruses (i.e., severe acute respiratory syndrome coronavirus [SARS-CoV], Middle East respiratory syndrome coronavirus [MERS-CoV], and severe acute respiratory syndrome coronavirus 2 [SARS-CoV-2]), swine-origin influenza A (H1N1), and e-cigarette or vaping product use–associated lung injury (EVALI). Because of their immature lung anatomy and developing immune systems, pediatric patients are often particularly susceptible to these public health crises. The ongoing SARS-CoV-2 outbreak, now deemed a global pandemic by the World Health Organization (WHO), has drawn attention to the importance of understanding the clinical and characteristic radiologic features of these lung disorders in the pediatric population.

Evaluation and diagnosis of pediatric lung disorders can be difficult because of the vague, overlapping nature of clinical symptoms, inability to communicate (in young or developmentally delayed infants and children), and nonspecific results often encountered during laboratory workup. Given the nonspecific nature of clinical presentation, imaging is an important component of diagnostic workup; thus, the radiologist plays an important role in initially detecting disease, evaluating response to treatment, and in some cases evaluating long-term sequelae of lung injury.

Although there are some overlapping imaging findings of these pediatric lung disorders, characteristic imaging features are currently emerging. This article provides an up-to-date review of the underlying causes, epidemiology, pertinent clinical presentation, and characteristic imaging findings of severe viral infections (i.e., SARS-CoV, MERS-CoV, SARS-CoV-2, and H1N1) and EVALI in pediatric patients with an emphasis on unique imaging features to help practicing radiologists accurately recognize and differentiate these novel lung disorders in the pediatric population.

Underlying Causes and Epidemiology

Coronaviruses: SARS-CoV, MERS-CoV, and SARS-CoV-2

First described in the 1960s as a cause for the common cold, human coronaviruses have become a global health threat in the 21st century after the emergence of severe respiratory syndromes associated with three coronaviruses: SARS-CoV, MERS-CoV, and SARS-CoV-2 [1, 2]. Coronaviruses are enveloped viruses with a single-stranded large RNA genome. The term "coronavirus" refers to the electron-microscopic appearance of the virions in which spike projections from the virus membrane resemble the appearance of a crown. Seven coronavi-

ruses are known to cause disease in humans with symptoms ranging from the common cold to severe, potentially fatal respiratory syndromes. SARS-CoV, MERS-CoV, and SARS-CoV-2 are the three coronaviruses that have resulted in contagious viral epidemics. The underlying causes and epidemiology are briefly discussed in the following sections, and the imaging findings of each coronavirus are discussed [2].

SARS-CoV—SARS-CoV was the first highly pathogenic coronavirus to infect humans and results in severe acute respiratory syndrome (SARS). It led to a pandemic of atypical pneumonia cases originating in Guangdong Province, China, in November 2002 [3]. The outbreak ultimately resulted in 8098 cases, 916 of which were fatal, across 29 countries in 2002–2003 before it was contained [4]. Although the exact causative origin of SARS-CoV remains uncertain, virology and genetics research has suggested zoonotic transmission from bats to palm civets and subsequently to humans [5].

SARS-CoV is spread predominantly through person-to-person contact via respiratory droplets. Once inside the respiratory tract, the virus binds to angiotensin-converting enzyme 2 (ACE2) receptor expressed by the epithelial cells of the alveoli, trachea, and bronchi as well as by alveolar macrophages and monocytes. The virus subsequently leads to a marked inflammatory response and increased vascular permeability, which leads to pneumonia and in some cases respiratory failure [4, 6].

MERS-CoV—First identified in Saudi Arabia in September 2012, Middle East respiratory syndrome (MERS) is a coronavirus-induced respiratory syndrome caused by MERS-CoV that resulted in an outbreak of atypical pneumonia and respiratory failure cases between 2012 and 2018. The pandemic led to 2254 cases of MERS and 800 deaths across 27 countries, although approximately 80% of the cases occurred in Saudi Arabia [4, 7]. The exact origin of the virus is still unclear; however, bats are favored to represent the natural host of MERS-CoV, similar to SARS-CoV, with dromedary camels, which are the only documented source for zoonotic transmission, acting as an intermediary [8].

Whereas SARS-CoV binds to the ACE2 receptor, MERS-CoV primarily binds to the cell surface protein dipeptidyl peptidase 4 (DDP4), which is abundant in the human respiratory tract including bronchial mucosa and alveoli. However, DDP4 is also expressed by epithelial cells in the kidneys, small intestines, liver, prostate, and activated leukocytes [4, 9]. MERS-CoV subsequently leads to immune dysregulation, which may then result in a delayed proinflammatory response in lung epithelial cells [4, 10].

SARS-CoV-2—Respiratory infection caused by the 2019 novel coronavirus (SARS-CoV-2) was first discovered in Wuhan, China, in December 2019. It has subsequently resulted in a global outbreak declared by the WHO to represent a pandemic on March 11, 2020 [11]. As of March 30, 2020, there have been 693,282 cases of coronavirus disease (COVID-19), the disease caused by SARS-CoV-2 infection, and 33,106 deaths across 202 countries and territories, including 122,653 cases and 2112 deaths in the United States [12].

Early data suggest that SARS-CoV-2 is more prevalent in male patients and that the highest levels of mortality occur in elderly patients and in those with preexisting comorbidities [13]. Health care workers are also at an elevated risk of SARS-CoV-2 infection, with up to 14.8% of 1716 confirmed cases in health care workers classified as severe or critical [14]. Children overall appear to be less severely affected than adults, with one study of 2143 children showing 94.1% of pediatric cases of COVID-19 to be asymptomatic, mild, or moderate [15]. The majority of pediatric COVID-19 cases affect children younger than 3 years old, with a slight male predominance [16]. The genetic sequence of SARS-CoV-2 is identical to more than 80% of the genetic sequence of SARS-CoV and 50% of the genetic sequence of MERS-CoV; zoonotic transmission with bats as the natural reservoir is favored to represent the origin of SARS-CoV-2, similar to both SARS-CoV and MERS-CoV [17].

Similar to SARS-CoV, SARS-CoV-2 has been shown to bind to ACE2 receptors within alveolar epithelial cells, leading to elevated levels of ACE2 and ultimately resulting in alveolar damage [13]. Elevated levels of proinflammatory cytokines in patients with COVID-19, greater in ICU patients than in non-ICU patients, suggest that immune dysregulation may also play a role in the disease pathogenesis [18].

H1N1

The H1N1 virus is a zoonotic virus that originated from pig-to-human transmission in Mexico in 2009 and consequently is also known as "swine-origin influenza A virus" or "S-OIV." This respiratory virus resulted in a pandemic in 2009 involving 214 countries and overseas territories [19]. Although 18,500 deaths due to laboratory-confirmed H1N1 were reported worldwide, the actual number of deaths due to H1N1 is estimated to be substantially higher because of undersampling and the fact that the virus was no longer detectable at the time of death in some patients [20]. In a modeling study by Dawood et al. [20], the global mortality during the first 12 months of the H1N1 pandemic was estimated at 201,200 respiratory-related deaths (range, 105,700–395,600 deaths) and 83,300 cardiovascular-related deaths (range, 46,000–179,900 deaths). In the United States, the estimated disease burden was 60.8 million cases (range, 43.3–89.3 million cases), resulting in approximately 274,304 hospitalizations (range, 195,086–402,719 hospitalizations) and 12,469 deaths (range, 8888–18,306 deaths) [21].

Influenza A is an enveloped single-stranded negative-sense RNA virus belonging to the Orthomyxoviridae family, which is subtyped according to two cell surface glycoproteins: hemagglutinin (16 types) and neuraminidase (nine types) [22]. Influenza A spreads via contact with aerosolized respiratory droplets or respiratory fomites from an infected individual. In humans, the respiratory epithelium is the only site where the hemagglutinin molecule is cleaved, leading to generation of infectious viral particles [23]. The virus causes local inflammation and compromise within the respiratory epithelium from direct viral invasion and triggers lung inflammation caused by the host immune response.

EVALI

Electronic cigarettes (e-cigarettes), also known as vapes, are battery-powered devices that can heat and aerosolize liquid combinations of nicotine, tetrahydrocannabinol, cannabinoid oils, flavors, and other additives (e.g., vitamin E) for inhalation. Increasingly popular among middle school–age children and high school–age adolescents, e-cigarettes have become the most commonly used tobacco product among U.S. teenagers and young adults since 2014 [24]. Unfortunately, EVALI cases spiked in late 2019, resulting in the Centers for Disease Control and Prevention deeming EVALI a national outbreak. As of February 18, 2020, there have been 2807 hospitalizations—including 68 deaths—due to EVALI across

TABLE 1: Imaging Findings in New Pediatric Lung Disorders

Lung Disorder	Chest Radiography	Chest CT	Helpful Imaging Features
SARS	Often normal findings; patchy opacities may be unilateral, especially during early stage; lower lung zone predominance; multifocal in one-third of cases	Unifocal or multifocal GGO, consolidation, or both; may be unilateral (early stage) or bilateral; peripheral or combined peripheral and central-distribution; mid and lower lung zones	Initially unifocal; peripheral or combined peripheral and central distribution; pleural effusion absent
MERS	Unifocal GGO in mid and lower lung zones but may progress to be multifocal, bilateral, or both; fine interstitial reticular pattern; pneumothorax or pleural effusion more common in fatal cases	Bilateral GGO with or without consolidation; peripheral and lower lung zone distribution; pleural effusion more common in fatal cases	Unifocal and unilateral (early stage); fine interstitial reticular pattern; pleural effusion and pneumothorax
COVID-19	May show normal findings; patchy bilateral GGO, consolidation, or both; peripheral and lower lung zone predominance	Bilateral multifocal GGO with or without consolidation, peripheral and subpleural distribution (often extending to pleural surface), possible halo sign Central distribution, pleural effusion, and lymphadenopathy are rarely seen and should prompt consideration of other differential diagnoses	Peripheral and subpleural distribution (often extending to pleural surface), halo sign Central distribution, pleural effusion, or lymphadenopathy suggests possible alternative diagnosis
H1N1	Often normal; in mild cases, bilateral hyperinflation and prominent peribronchial markings; in moderate and severe cases, one or more areas of GGO, consolidation, or both in bilateral symmetric distribution	Bronchovascular thickening; bilateral multifocal central lung–predominant GGO, consolidation, or both; possible pneumomediastinum	Bilateral hyperinflation and bronchovascular thickening (early stage); bilateral symmetric multifocal GGO, consolidation, or both (late stage); central distribution
EVALI	Bilateral multifocal GGO, consolidation, or both; symmetric; lower lung zones; possible subpleural sparing	Bilateral symmetric GGO with or without consolidation; subpleural sparing; mild lower lobe predominance; possible centrilobular nodules; possible atoll sign	Subpleural sparing; atoll sign

Note—SARS = severe acute respiratory syndrome, GGO = ground-glass opacity, MERS = Middle East respiratory syndrome, COVID-19 = coronavirus disease (2019), H1N1 = swine-origin influenza A, EVALI = e-cigarette or vaping product use–associated lung injury.

all 50 states, the District of Columbia, Puerto Rico, and the U.S. Virgin Islands [24].

Although the exact pathophysiology of EVALI is incompletely understood and is an active area of ongoing research, vitamin E acetate (VEA), also known as α-tocopherol acetate, an additive used as a carrier for drug delivery, is likely a contributor to the development of EVALI [25]. Strong support for this argument has been provided by Blount et al. [26], who evaluated bronchoalveolar lavage samples and found VEA in 48 of 51 samples from patients with EVALI compared with 0 of 99 healthy comparators including nonusers, nicotine-exclusive e-cigarette users, and cigarette smokers. Alterations in surfactant surface tension and production of the reactive compound ketene, which may serve as a lung irritant, during heating have been suggested as possible mechanisms of VEA-induced lung injury [26].

Characteristic Imaging Findings

Although the clinical symptoms and imaging findings of these new pediatric lung disorders may be nonspecific, some characteristic imaging features have emerged or are currently emerging. These imaging findings are summarized by lung disorder in Table 1.

SARS

Pediatric patients with SARS tend to have a milder clinical course than adults with SARS, with up to 35% of pediatric patients with SARS found to have normal findings on chest radiographs [27]. In pediatric SARS cases with a radiographic abnormality, the most frequently observed findings are patchy ground-glass opacities (GGOs) and areas of consolidation predominantly in lower lung zones, with multifocal involvement in up to one-third of affected patients [27, 28] (Figs. 1A and 1B). Cavitation, pleural effusion, and lymphadenopathy are generally absent [29–31].

CT is more sensitive than radiography for the detection of parenchymal abnormalities in patients with SARS and frequently shows parenchymal abnormalities when initial chest radiographs show normal findings [29]. In pediatric patients, the most common CT findings during the acute period of SARS are unifocal or multifocal central or peripheral consolidations and GGOs [27] (Fig. 1C). The extent of parenchymal injury visible on CT is often greater than that appreciated radiographically. Chu et al. [32] evaluated the delayed manifestations of SARS in 47 pediatric patients 6 and 12 months after SARS-CoV diagnosis and found that the majority of patients (66%) had no imaging abnormalities at 6 months. The most common abnormalities observed at 6 months were persistent GGOs, air trapping, and small parenchymal scars. By 12 months after SARS-CoV diagnosis, GGOs had improved or resolved in all cases, but lower lobe–predominant subsegmental and subpleural air trapping and small parenchymal scars persisted in all cases [32].

MERS

MERS has a nonspecific presentation of fever, difficulty breathing, and cough among the most common clinical symptoms. Chest radiography is an important tool both in initial evaluation and in tracking disease progression because mean chest radiographic score is an independent predictor of mortality. Furthermore, a static radiographic pattern of lung changes over time is associated with the highest rate of pulmonary fibrotic change, and a progressive radiographic pattern has been associated with a higher mortality rate [33, 34].

The most frequently observed chest radiography findings in patients with MERS are unifocal GGOs in the mid and lower lung zones, which may eventually progress to multifocal and bilateral airspace opacities as the disease

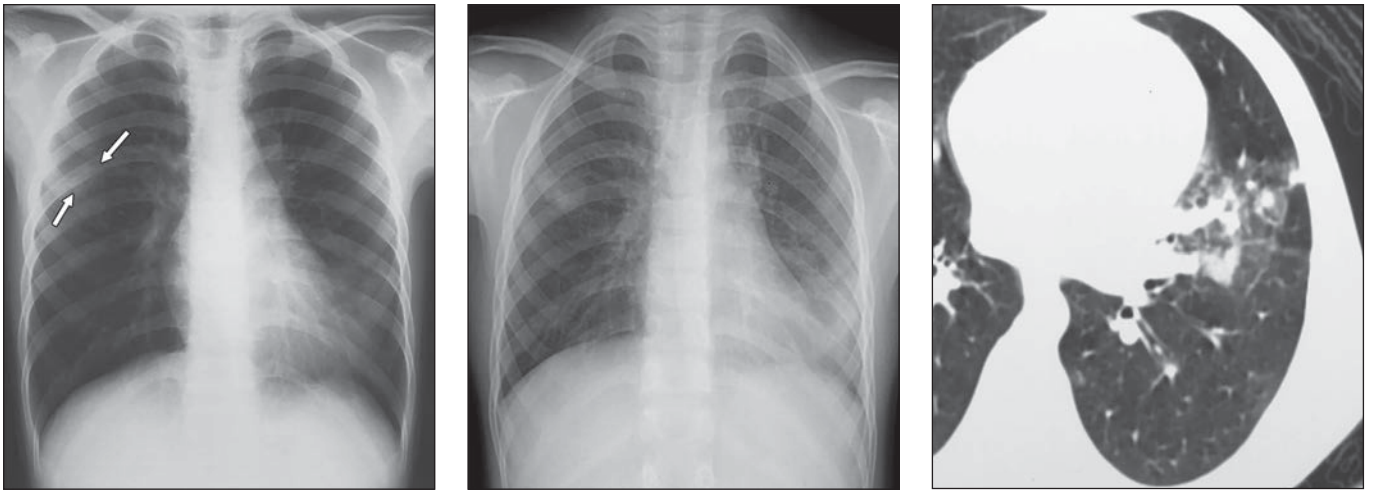

Fig. 1—8-year-old boy with severe acute respiratory syndrome who presented to hospital with 5-day history of fever, chills, and rigor.
A, Frontal chest radiograph shows ill-defined airspace consolidation in lingula with loss of left heart border. Another smaller area of airspace opacification (*arrows*) is present in right upper lung zone.
B, Frontal chest radiograph obtained 2 days after initial chest radiograph (**A**) shows increase in extent of airspace opacification in both lingula and right upper lung zone.
C, Axial lung window setting CT image obtained 7 days after hospital admission shows mixed airspace consolidation and ground-glass opacity in lingula.

progresses [33, 35, 36] (Fig. 2). Although less frequently observed, pneumothorax or pleural effusion is significantly more common in fatal cases of MERS and, consequently, is an important observation for the radiologist to make [33]. Very few pediatric cases of MERS have been reported in the literature; however, a fine interstitial reticular pattern of interstitial inflammation has been described [37].

On CT, the most frequently observed pattern is GGOs alone or in combination with consolidation in a peripheral and basilar distribution involving multiple lung segments, often bilaterally [38, 39] (Fig. 3). The observation of multisegmental or bilateral involvement on CT likely relates to the CT examination being performed mainly in more seriously ill patients and often several days into the course of illness. Interlobular septal thickening and pleural effusion have also been described, the latter of which was observed in only fatal cases in one study [38].

Coronavirus Disease (COVID-19)

The clinical presentation of COVID-19 is relatively nonspecific with fever, cough, myalgia, and fatigue representing the most common presenting features. Similarly, laboratory values overall have proven relatively nonspecific, although multiple studies have reported lymphopenia, leukopenia, thrombocytopenia, elevated C-reactive protein, and elevated erythrocyte sedimentation rate [40–45]. Thus, chest imaging, whether chest radiography or cross-section imaging such as CT, plays an important role in the diagnostic workup of suspected COVID-19. Furthermore, both the limited supply of reverse transcription–polymerase chain reaction (RT-PCR) tests for detecting SARS-CoV-2 and somewhat high false-negative rate of RT-PCR tests for detecting SARS-CoV-2 can lead to delayed treatment. Chest CT has been shown to have a significantly higher rate of sensitivity in detection of SARS-CoV-2 than the initial RT-PCR test [46, 47]. In fact, during the peak outbreak in China, chest CT findings were added as major evidence for confirmed clinical diagnosis [48].

In most institutions, chest radiography is the first imaging study performed in patients with clinically suspected COVID-19. Despite this fact, the studies in the literature on chest radiography findings in patients with COVID-19 are relatively scarce. Yoon et al. [49] reported patchy, bilateral, peripheral lower lung zone–predominant consolidations and, to a lesser extent, GGOs on chest radiographs in three of nine adult patients with laboratory-confirmed SARS-CoV-2 in-

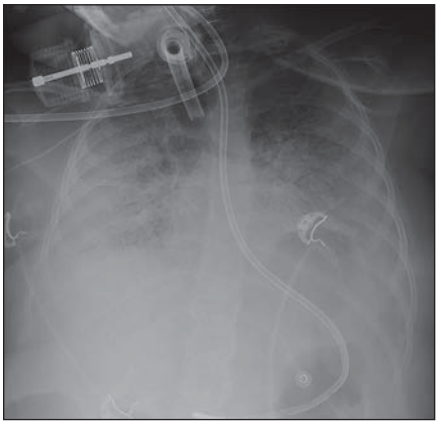

Fig. 2—12-year-old boy with Middle East respiratory syndrome who presented with severe respiratory distress and hypoxia. Frontal chest radiograph shows bilateral consolidations and ground-glass opacities in lung periphery–predominant distribution. Also noted are tracheostomy tube and nasogastric tube.

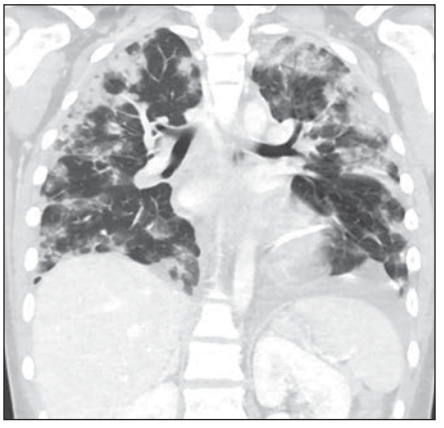

Fig. 3—20-year-old man with Middle East respiratory syndrome who presented with difficulty breathing and cough. Coronal lung window setting CT image shows bilateral ground-glass opacities and consolidations in peripheral distribution.

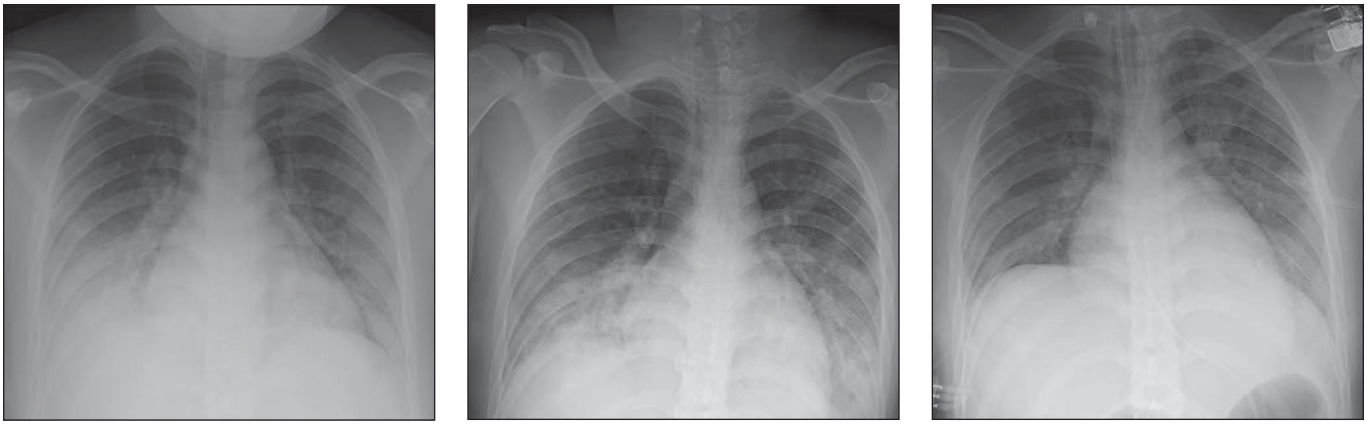

Fig. 4—16-year-old girl with coronavirus disease (COVID-19) and known history of tuberous sclerosis who presented with acute hypoxic respiratory distress. Reverse transcription–polymerase chain reaction testing confirmed diagnosis of severe acute respiratory syndrome coronavirus 2 (SARS-CoV-2).
A, Frontal chest radiograph obtained at initial presentation shows bilateral lower lung zone–predominant consolidations and, to lesser extent, ground-glass opacities.
B, Frontal chest radiograph obtained 2 days after hospital admission shows interval increase in consolidation in bilateral lower lung zones.
C, Frontal chest radiograph obtained 6 days after hospital admission and treatment shows interval improvement in consolidations in bilateral lower lung zones.

fection (Fig. 4). However, in the same cohort of patients, chest CT showed lung parenchymal abnormalities in eight of nine patients [49]. A small subset of five patients, in a larger study of 21 patients with COVID-19 [50], underwent both chest radiography and chest CT examinations. Radiography and CT revealed consolidative opacities in three of the five patients, one with lower zone predominance and two without zonal predominance; however, the peripheral predominance of the opacity observed on CT was not seen on chest radiography. The remaining two patients had negative findings on chest radiography but were found to have lung periphery–predominant GGOs on chest CT [50]. In a case series of 10 pediatric COVID-19 cases in China, investigators reported unilateral patchy opacities on chest radiographs in four of 10 cases but did not describe the imaging characteristics in detail [51].

The studies in the literature describing chest CT findings in patients with COVID-19 are more robust than those describing the chest radiography findings. The most frequently observed pattern of lung disease seen on CT in adult patients is bilateral multifocal GGOs alone or in combination with consolidations in a peripheral or subpleural distribution [43, 45, 46, 49, 52–55]. When compared with cases of non–COVID-19 pneumonia, COVID-19 pneumonia cases have been found to have significantly more air bronchograms, increased frequency of reticular pattern, more peripheral distribution of airspace opacities, and increased numbers of lung segments and lobes involved on CT, were more likely to have vascular thickening, and were more likely to have a "reversed halo" sign present on CT [56, 57]. Patients with COVID-19 pneumonia were significantly less likely to have centrilobular nodules, central distribution, and extrapulmonary abnormalities, such as pleural effusion or lymphadenopathy [56, 57]. A few studies have reported early temporal imaging findings in the acute to subacute phase of SARS-CoV-2 infection, describing an initial increase in GGOs over time and, as might be expected, signs of early organization, including increased reticulation, architectural distortion, bronchus distortion, and fibrotic streaks [43, 44, 58].

Only a few articles have reported CT findings of COVID-19 in children. Xia et al. [41] reported that the most frequently observed abnormalities on CT in 20 pediatric patients with COVID-19 were subpleural lesions (100% of patients), unilateral (30%) or bilateral (50%) pulmonary lesions, GGO (60%), and consolidation with a rim of GGO surrounding it, also known as the halo sign (50%) (Fig. 5). In a smaller study of five pediatric patients with COVID-19, investigators reported modest patchy GGO, one with peripheral subpleural involvement, in three patients that resolved on follow-up CT examination [59].

H1N1

H1N1 presents with nonspecific symptoms including fever, cough, and myalgia, which are the most common symptoms, and dyspnea, which has been reported as occurring occasionally. Both radiographic and CT abnormalities have been shown to correlate with worse clinical outcomes; thus, radiologic evaluation plays an important role in diagnosis and prognostication in these patients [60].

In both pediatric and adult populations, chest radiography findings are normal in

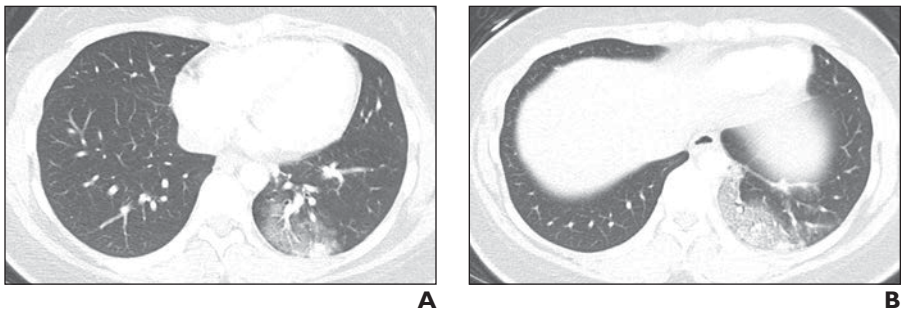

Fig. 5—16-year-old girl with coronavirus disease (COVID-19) who presented with shortness of breath. Reverse transcription–polymerase chain reaction testing confirmed diagnosis of severe acute respiratory syndrome coronavirus 2 (SARS-CoV-2).
A–D, Axial (**A** and **B**), coronal (**C**), and sagittal (**D**) lung window setting CT images show posterior subpleural ground-glass opacity with small component of consolidation within left lower lobe.

(Fig. 5 continues on next page)

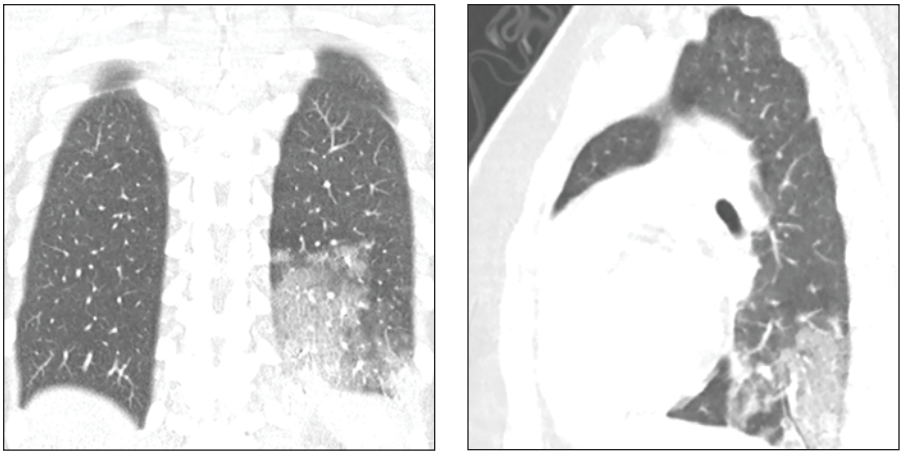

Fig. 5 (continued)—16-year-old girl with coronavirus disease (COVID-19) who presented with shortness of breath. Reverse transcription–polymerase chain reaction testing confirmed diagnosis of severe acute respiratory syndrome coronavirus 2 (SARS-CoV-2).
A–D, Axial (**A** and **B**), coronal (**C**), and sagittal (**D**) lung window setting CT images show posterior subpleural ground-glass opacity with small component of consolidation within left lower lobe.

a large number of H1N1 cases [60–64]. In adults with H1N1 who are found to have a radiographic abnormality, the most common findings are bilateral patchy and nodular opacities in the mid and lower lung zones [61, 64–66]. In mild cases of H1N1 in pediatric patients, the most frequently observed imaging abnormalities are prominent peribronchial markings and hyperinflation (Fig. 6). Chest radiographs of pediatric patients with H1N1 who require hospitalization may reveal one or more areas of consolidation or GGO, typically in a bilateral symmetric distribution without a zonal preference [62] (Fig. 7). Bilateral peribronchovascular opacities and consolidative opacity or GGO in an asymmetric or lower lung–predominant distribution have also been described [63, 67].

CT of the chest in adult patients with H1N1 typically shows peribronchial thickening, bilateral GGOs or consolidation, and nodular opacities in a central and peripheral peribronchovascular or diffuse distribution [60, 61, 64, 68]. Interlobular septal thickening, reticulation, pleural effusions, and mediastinal lymphadenopathy may be observed in nearly one-fourth of patients [69]. CT examinations are performed in pediatric patients less frequently than in adults, likely because of a combination of less severe clinical course in pediatric patients and concerns regarding radiation exposure. When chest CT is performed, the most common findings in pediatric patients with H1N1 are bilateral, multifocal, central lung–predominant consolidation or GGOs and bronchovascular thickening [70]. In addition, it is interesting that pneumomediastinum has been observed in several H1N1 cases in pediatric patients [63, 70, 71].

EVALI

EVALI is an important differential consideration in the pediatric population given that up to 50% of EVALI cases occur in patients younger than 21 years old. Furthermore, the clinical presentation, which typically includes constitutional, respiratory, and gastrointestinal symptoms, is nonspecific and overlaps with symptoms observed in other infectious entities. The radiologist may be the first to raise this diagnostic possibility, which can lead to acquisition of a more detailed social history and, in some cases, to altered management.

Chest radiographs of both pediatric and adult populations typically show bilateral multifocal GGO or consolidation in a symmetric pattern predominantly in the lower lung zones [72–75]. Sparing of the subpleural and pericardiac region may be observed [75]. Pneumomediastinum and pneumothorax have also been reported in a few cases [72, 76, 77].

Chest CT of adult patients with EVALI most often shows bilateral multifocal GGOs, consolidation, or both, frequently with subpleural sparing [75, 77]. However, multiple distinct imaging patterns have been reported, including acute eosinophilic pneumonia, diffuse alveolar damage, organizing pneumonia, hypersensitivity pneumonitis, lipoid pneumonia, diffuse alveolar hemorrhage, and, in at least one case, giant cell interstitial pneumonia [73–75, 78–82]. In pediatric patients, CT often shows bilateral symmetric GGOs with or without consolidation with subpleural sparing and a slight lower lobe predominance [72, 83]. Centrilobular ground-glass nodules may also be observed [72, 83]. Although not present in all cases, the "atoll" sign (i.e., central GGO surrounded by dense consolidation of crescentic shape) has been described in up to 36% of

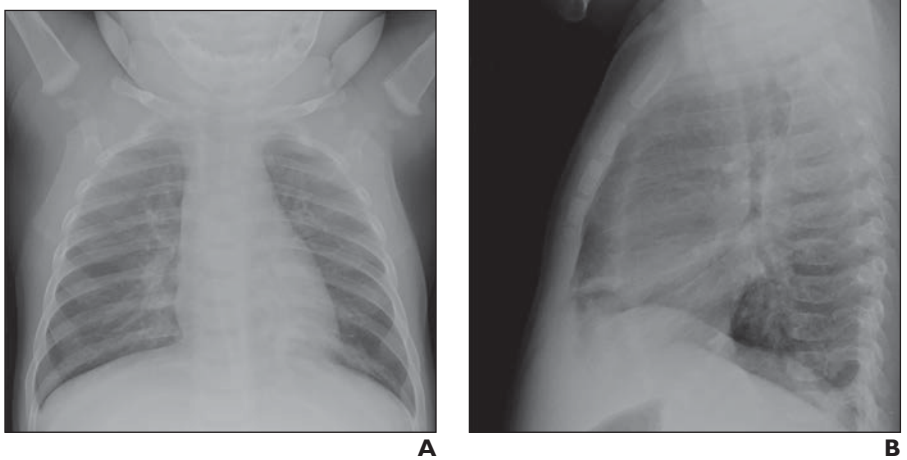

Fig. 6—7-month-old boy with swine-origin influenza A (H1N1) who presented with fever and cough. Viral direct fluorescent antibody test results were positive for H1N1 and negative for respiratory syncytial virus; influenza B; adenovirus; and parainfluenza viruses 1, 2, and 3.
A and **B,** Frontal (**A**) and lateral (**B**) chest radiographs show hyperinflation and bilateral prominent peribronchial markings.

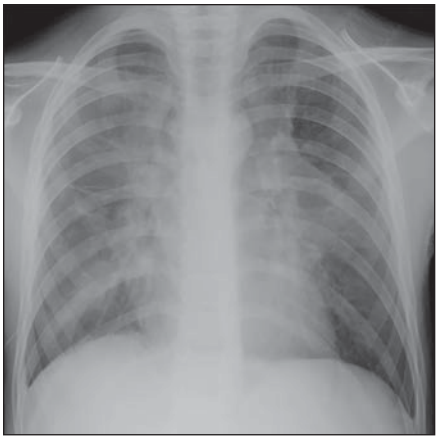

Fig. 7—6-year-old boy with swine-origin influenza A (H1N1) and known asthma who presented with cough and myalgia. Viral direct fluorescent antibody test results were positive for H1N1 and negative for respiratory syncytial virus; influenza B; adenovirus; and parainfluenza viruses 1, 2, and 3. Frontal chest radiograph shows consolidations and ground-glass opacities in upper, mid, and lower zones of both lungs in bilateral, symmetric, and central distribution.

cases and may prove helpful in narrowing the differential diagnosis [72] (Fig. 8).

Future Directions

Early recognition of imaging characteristics of specific pediatric lung disorders, including severe viral infections and EVALI, is key to making a timely and accurate diagnosis. These lung disorders are often difficult to study in children given that the affected pediatric patient population may be small. In the future, a multicenter effort to increase sample size and allow improved characterization during the early phase of disease development is essential. Therefore, close

Fig. 8—17-year-old boy with history of e-cigarette or vaping product use–associated lung injury (EVALI) who presented with shortness of breath and cough for 4 weeks. Axial lung window setting CT image shows bilateral ground-glass opacities with subpleural sparing (*arrowheads*). Peripheral ring of consolidation with surrounding ground-glass opacity and central lucency is seen in right lung in keeping with "atoll" sign (*asterisk*).

communication and collaboration among international pediatric thoracic radiologists is important. In addition, collaboration with other pediatric specialists, such as pediatric surgeons who can perform lung biopsy in patients with suspected EVALI and pediatric pathologists who can provide histologic correlation, is imperative to gain a better understanding of the pathogenesis of the imaging abnormalities observed in these disorders.

Cross-sectional imaging, such as chest CT, can provide improved characterization of lung abnormalities in pediatric lung disorders; however, the studies in the literature describing the CT findings in pediatric patients are scarce, presumably because of the concerns about the harmful effects of ionizing radiation [84]. Fortunately, there have been substantial improvements in lung MRI technique in recent years with motion correction and parallel imaging [85–87]. Lung MRI may be helpful and can provide additional structural and functional information without associated ionizing radiation; however, future studies are needed to assess the utility of MRI in identifying markers for pediatric lung disorders.

Conclusion

The clinical presentation and laboratory evaluation of pediatric patients presenting with several relatively new lung disorders are often nonspecific with a great deal of overlap. A clear understanding of the imaging manifestations of these pediatric lung disorders is essential so that the radiologist can make a timely and accurate diagnosis (Table 2). Although there are some overlapping imaging features of these disorders, careful evaluation of the distribution, lung zone preference, and symmetry of the abnormalities with an eye for a few unique differentiating imaging features, such as the halo sign seen in COVID-19 and subpleural sparing and the atoll sign seen in EVALI, can allow the radiologist to offer a narrower differential diagnosis in pediatric patients, leading to optimal patient care.

References

1. Willman M, Kobasa D, Kindrachuk J. A comparative analysis of factors influencing two outbreaks of Middle Eastern respiratory syndrome (MERS) in Saudi Arabia and South Korea. *Viruses* 2019; 11:E1119
2. Su S, Wong G, Shi W, et al. Epidemiology, genetic recombination, and pathogenesis of coronaviruses. *Trends Microbiol* 2016; 24:490–502
3. Zhong NS, Zheng BJ, Li YM, et al. Epidemiology

TABLE 2: What Radiologists Need to Know About Severe Acute Respiratory Syndrome (SARS), Middle East Respiratory Syndrome (MERS), Coronavirus Disease (COVID-19), Swine-Origin Influenza A (H1N1), and E-Cigarette or Vaping Product Use–Associated Lung Injury (EVALI)

Lung Disorder	Imaging Characteristics
SARS	Often initially presents with unifocal GGO, consolidation, or both in the lower lung zone in a peripheral or combined peripheral and central distribution
MERS	May initially present with unifocal GGO, consolidation, or both in a peripheral and lower lung zone distribution; pleural effusion or pneumothorax may be observed and is suggestive of a more severe clinical course
COVID-19	Frequently presents with bilateral multifocal GGO, often with associated consolidation, in a peripheral and subpleural distribution; halo sign may also be seen; central distribution, pleural effusion, and lymphadenopathy are rare and, when present, should lead to a broadened differential diagnosis
H1N1	Mild cases typically present with normal findings on chest radiography or hyperinflation with prominent bilateral symmetric peribronchial markings; severe cases show bilateral central lung–predominant GGO, consolidation, or both
EVALI	Most commonly presents with multifocal bilateral symmetric GGO, consolidation, or both, frequently with subpleural sparing; "atoll" sign may be seen and, when present, can help narrow the differential diagnosis

Note—GGO = ground-glass opacity.

and cause of severe acute respiratory syndrome (SARS) in Guangdong, People's Republic of China, in February, 2003. *Lancet* 2003; 362:1353–1358

4. Song Z, Xu Y, Bao L, et al. From SARS to MERS, thrusting coronaviruses into the spotlight. *Viruses* 2019; 11:E59
5. Shi Z, Hu Z. A review of studies on animal reservoirs of the SARS coronavirus. *Virus Res* 2008; 133:74–87
6. de Wit E, van Doremalen N, Falzarano D, Munster VJ. SARS and MERS: recent insights into emerging coronaviruses. *Nat Rev Microbiol* 2016; 14:523–534
7. World Health Organization website. WHO MERS-CoV global summary and assessment of risk. www.who.int/docs/default-source/documents/health-topics/mers/mers-summary-5december2016.pdf?sfvrsn=f061dca9_1. Published December 5, 2016. Accessed March 21, 2020
8. Dawson P, Malik MR, Parvez F, Morse SS. What have we learned about Middle East respiratory syndrome coronavirus emergence in humans? A systematic literature review. *Vector Borne Zoonotic Dis* 2019; 19:174–192
9. Widagdo Q, Raj VS, Schipper D, et al. Differential expression of the Middle East respiratory syndrome coronavirus receptor in the upper respiratory tracts of humans and dromedary camels. *J Virol* 2016; 90:4838–4842
10. Yin Y, Wunderink RG. MERS, SARS and other coronaviruses as causes of pneumonia. *Respirology* 2018; 23:130–137
11. World Health Organization website. Coronavirus disease 2019 (COVID-19): situation report 51. www.who.int/docs/default-source/coronaviruse/situation-reports/20200311-sitrep-51-covid-19.pdf?sfvrsn=1ba62e57_10. Published March 11, 2020. Accessed March 22, 2020
12. World Health Organization website. Coronavirus disease 2019 (COVID-19): situation report 73. www.who.int/docs/default-source/coronaviruse/situation-reports/20200402-sitrep-73-covid-19.pdf?sfvrsn=5ae25bc7_4. Published April 2, 2020. Accessed April 2, 2020
13. Sun P, Lu X, Xu C, Sun W, Pan B. Understanding of COVID-19 based on current evidence. *J Med Virol* 2020 Feb 25 [Epub ahead of print]
14. Wu Z, McGoogan JM. Characteristics of and important lessons from the coronavirus disease 2019 (COVID-19) outbreak in China: summary of a report of 72 314 cases from the Chinese Center for Disease Control and Prevention. *JAMA* 2020 Feb 24 [Epub ahead of print]
15. Dong Y, Mo X, Hu Y, et al. Epidemiological characteristics of 2143 pediatric patients with 2019 coronavirus disease in China. *Pediatrics* 2020 Mar 16 [Epub ahead of print]
16. Zheng F, Liao C, Fan Q, et al. Clinical characteristics of children with coronavirus disease 2019 in Hubei, China. *Curr Med Sci* 2020 Mar 24 [Epub ahead of print]
17. Rothan HA, Byrareddy SN. The epidemiology and pathogenesis of coronavirus disease (COVID-19) outbreak. *J Autoimmun* 2020 Feb 26 [Epub ahead of print]
18. Huang C, Wang Y, Li X, et al. Clinical features of patients infected with 2019 novel coronavirus in Wuhan, China. *Lancet* 2020; 395:497–506
19. World Health Organization website. Pandemic (H1N1) 2009: update 112. www.who.int/csr/don/2010_08_06/en/. Published August 6, 2010. Accessed March 22, 2020
20. Dawood FS, Iuliano AD, Reed C, et al. Estimated global mortality associated with the first 12 months of 2009 pandemic influenza A H1N1 virus circulation: a modelling study. *Lancet Infect Dis* 2012; 12:687–695
21. Shrestha SS, Swerdlow DL, Borse RH, et al. Estimating the burden of 2009 pandemic influenza A (H1N1) in the United States (April 2009-April 2010). *Clin Infect Dis* 2011; 52(suppl 1):S75–S82
22. Labella AM, Merel SE. Influenza. *Med Clin North Am* 2013; 97:621–645
23. Kalil AC, Thomas PG. Influenza virus-related critical illness: pathophysiology and epidemiology. *Crit Care* 2019; 23:258
24. Centers for Disease Control and Prevention website. Outbreak of lung injury associated with the use of e-cigarette, or vaping, products. www.cdc.gov/tobacco/basic_information/e-cigarettes/severe-lung-disease.html. Published February 25, 2020. Accessed March 22, 2020
25. Chand HS, Muthumalage T, Maziak W, Rahman I. Pulmonary toxicity and the pathophysiology of electronic cigarette, or vaping product, use associated lung injury. *Front Pharmacol* 2020; 10:1619
26. Blount BC, Karwowski MP, Shields PG, et al.; Lung Injury Response Laboratory Working Group. Vitamin E acetate in bronchoalveolar-lavage fluid associated with EVALI. *N Engl J Med* 2020; 382:697–705
27. Babyn PS, Chu WCW, Tsou IYY, et al. Severe acute respiratory syndrome (SARS): chest radiographic features in children. *Pediatr Radiol* 2004; 34:47–58
28. Tsou IY, Loh LE, Kaw GJ, Chan I, Chee TS. Severe acute respiratory syndrome (SARS) in a paediatric cluster in Singapore. *Pediatr Radiol* 2004; 34:43–46
29. Müller NL, Ooi GC, Khong PL, Zhou LJ, Tsang KW, Nicolaou S. High-resolution CT findings of severe acute respiratory syndrome at presentation and after admission. *AJR* 2004; 182:39–44
30. Ooi GC, Daqing M. SARS: radiological features. *Respirology* 2003; 8(suppl):S15–S19
31. Ooi GC, Khong PL, Müller NL, et al. Severe acute respiratory syndrome: temporal lung changes at thin-section CT in 30 patients. *Radiology* 2004; 230:836–844
32. Chu WC, Li AM, Ng AWH, et al. Thin-section CT 12 months after the diagnosis of severe acute respiratory syndrome in pediatric patients. *AJR* 2006; 186:1707–1714
33. Das KM, Lee EY, Al Jawder SE, et al. Acute Middle East respiratory syndrome coronavirus: temporal lung changes observed on the chest radiographs of 55 patients. *AJR* 2015; 205:[web] W267–W274
34. Das KM, Lee EY, Singh R, et al. Follow-up chest radiographic findings in patients with MERS-CoV after recovery. *Indian J Radiol Imaging* 2017; 27:342–349
35. Das KM, Lee EY, Langer RD, Larsson SG. Middle East respiratory syndrome coronavirus: what does a radiologist need to know? *AJR* 2016; 206:1193–1201
36. Cha MJ, Chung MJ, Kim K, Lee KS, Kim TJ, Kim TS. Clinical implication of radiographic scores in acute Middle East respiratory syndrome coronavirus pneumonia: report from a single tertiary-referral center of South Korea. *Eur J Radiol* 2018; 107:196–202
37. Das KM, Lee EY. Middle East respiratory syndrome coronavirus in children. *Indian Pediatr* 2016; 53:752
38. Das KM, Lee EY, Enani MA, et al. CT correlation with outcomes in 15 patients with acute Middle East respiratory syndrome coronavirus. *AJR* 2015; 204:736–742
39. Ajlan AM, Ahyad RA, Jamjoom LG, Alharthy A, Madani TA. Middle East respiratory syndrome coronavirus (MERS-CoV) infection: chest CT findings. *AJR* 2014; 203:782–787
40. Li LQ, Huang T, Wang YQ, et al. COVID-19 patients' clinical characteristics, discharge rate, and fatality rate of meta-analysis. *J Med Virol* 2020 Mar 12 [Epub ahead of print]
41. Xia W, Shao J, Guo Y, Peng X, Li Z, Hu D. Clinical and CT features in pediatric patients with COVID-19 infection: different points from adults. *Pediatr Pulmonol* 2020 Mar 5 [Epub ahead of print]
42. Chen ZM, Fu JF, Shu Q, et al. Diagnosis and treatment recommendations for pediatric respiratory infection caused by the 2019 novel coronavirus. *World J Pediatr* 2020 Feb 5 [Epub ahead of print]
43. Xu X, Yu C, Qu J, et al. Imaging and clinical features of patients with 2019 novel coronavirus SARS-CoV-2. *Eur J Nucl Med Mol Imaging* 2020; 47:1275–1280
44. Zhou S, Wang Y, Zhu T, Xia L. CT features of coronavirus disease 2019 (COVID-19) pneumonia in 62 patients in Wuhan, China. *AJR* 2020 Mar 5 [Epub ahead of print]
45. Han R, Huang L, Jiang H, Dong J, Peng H, Zhang

D. Early clinical and CT manifestations of coronavirus disease 2019 (COVID-19) pneumonia. *AJR* 2020 Mar 17 [Epub ahead of print]

46. Fang Y, Zhang H, Xie J, et al. Sensitivity of chest CT for COVID-19: comparison to RT-PCR. (*Radiology* 2020 Feb 19 [Epub ahead of print]
47. Ai T, Yang Z, Hou H, et al. Correlation of chest CT and RT-PCR testing in coronavirus disease 2019 (COVID-19) in China: a report of 1014 cases. *Radiology* 2020 Feb 26 [Epub ahead of print]
48. Zu ZY, Jiang MD, Xu PP, et al. Coronavirus disease 2019 (COVID-19): a perspective from China. *Radiology* 2020 Feb 21 [Epub ahead of print]
49. Yoon SH, Lee KH, Kim JY, et al. Chest radiographic and CT findings of the 2019 novel coronavirus disease (COVID-19): analysis of nine patients treated in Korea. *Korean J Radiol* 2020; 21:494–500
50. Ng MY, Lee EY, Yang J, et al. Imaging profile of the COVID-19 infection: radiologic findings and literature review. *Radiol Cardiothorac Imaging* 2020 Feb 13 [Epub ahead of print]
51. Cai J, Xu J, Lin D, et al. A case series of children with 2019 novel coronavirus infection: clinical and epidemiological features. *Clin Infect Dis* 2020 Feb 28 [Epub ahead of print]
52. Chung M, Bernheim A, Mei X, et al. CT imaging features of 2019 novel coronavirus (2019-nCoV). *Radiology* 2020; 295:202–207
53. Pan Y, Guan H, Zhou S, et al. Initial CT findings and temporal changes in patients with the novel coronavirus pneumonia (2019-nCoV): a study of 63 patients in Wuhan, China. *Eur Radiol* 2020 Feb 13 [Epub ahead of print]
54. Zhao W, Zhong Z, Xie X, Yu Q, Liu J. Relation between chest CT findings and clinical conditions of coronavirus disease (COVID-19) pneumonia: a multicenter study. *AJR* 2020 Mar 3 [Epub ahead of print]
55. Bernheim A, Mei X, Huang M, et al. Chest CT findings in COVID-19. *Radiology* 2020 Feb 20 [Epub ahead of print]
56. Cheng Z, Lu Y, Cao Q, et al. Clinical features and chest CT manifestations of coronavirus disease 2019 (COVID-19) in a single-center study in Shanghai, China. *AJR* 2020 Mar 14 [Epub ahead of print]
57. Bai HX, Hsieh B, Xiong Z, et al. Performance of radiologists in differentiating COVID-19 from viral pneumonia on chest CT. *Radiology* 2020 Mar 10 [Epub ahead of print]
58. Wang Y, Dong C, Hu Y, et al. Temporal changes of CT findings in 90 patients with COVID-19 pneumonia: a longitudinal study. *Radiology* 2020 Mar 19 [Epub ahead of print]
59. Li W, Cui H, Li K, Fang Y, Li S. Chest computed tomography in children with COVID-19 respiratory infection. *Pediatr Radiol* 2020 Mar 11 [Epub ahead of print]
60. Schoen K, Horvat N, Guerreiro NFC, de Castro I, de Giassi KS. Spectrum of clinical and radiographic findings in patients with diagnosis of H1N1 and correlation with clinical severity. *BMC Infect Dis* 2019; 19:964
61. Agarwal PP, Cinti S, Kazerooni EA. Chest radiographic and CT findings in novel swine-origin influenza A (H1N1) virus (S-OIV) infection. *AJR* 2009; 193:1488–1493
62. Lee EY, McAdam AJ, Chaudry G, Fishman MP, Zurakowski D, Boiselle PM. Swine-origin influenza a (H1N1) viral infection in children: initial chest radiographic findings. *Radiology* 2010; 254:934–941
63. Choi MJ, Lee YS, Lee JY, Lee KS. Novel influenza A (H1N1) virus infection in children: chest radiographic and CT evaluation. *Korean J Radiol* 2010; 11:656–664
64. Yun TJ, Park CM, Kwon GJ, et al. Clinical and radiological features of pandemic H1N1 2009 influenza virus infection manifesting as acute febrile respiratory illness at their initial presentations: comparison with contemporaneous non-H1N1 patients. *Acta Radiol* 2011; 52:410–416
65. Rohani P, Jude CM, Chan K, Barot N, Kamangar N. Chest radiological findings of patients with severe H1N1 pneumonia requiring intensive care. *J Intensive Care Med* 2016; 31:51–60
66. Minns FC, Mhuineachain AN, van Beek EJR, Ritchie G, Hill A, Murchison JT. Presenting CXR phenotype of H1N1 flu compared with contemporaneous non-H1N1, community acquired pneumonia, during pandemic and post-pandemic outbreaks. *Eur J Radiol* 2015; 84:1810–1815
67. Adôrno IF, Tibana TK, Santos RFT, et al. Initial chest X-ray findings in pediatric patients diagnosed with H1N1 virus infection. *Radiol Bras* 2019; 52:78–84
68. Göya C, Yavuz A, Hamidi C, et al. The role of initial radiologic and clinical manifestations in predicting the prognosis for pneumonia caused by H1N1 influenza virus. *J Thorac Dis* 2014; 6:752–759
69. Kang H, Lee KS, Jeong YJ, Lee HY, Kim KI, Nam KJ. Computed tomography findings of influenza A (H1N1) pneumonia in adults: pattern analysis and prognostic comparisons. *J Comput Assist Tomogr* 2012; 36:285–290
70. Yamada K, Shinmoto H, Hamamoto M, et al. Pneumonia induced by swine-origin influenza A (H1N1) infection: chest computed tomography findings in children. *Jpn J Radiol* 2011; 29:712–717
71. Yoshinobu T, Abe K, Shimizu H, Yokoyama M, Osawa M, Hiraishi Y. CT findings in pediatric novel influenza A (H1N1)-associated pneumonia. *Iran J Pediatr* 2012; 22:213–217
72. Artunduaga M, Rao D, Friedman J, et al. Pediatric chest radiographic and CT findings of electronic cigarette or vaping product use-associated lung injury (EVALI). *Radiology* 2020 Mar 3 [Epub ahead of print]
73. Sechrist JW, Kanne JP. Vaping-associated lung disease. *Radiology* 2020; 294:18
74. Khan MS, Khateeb F, Akhtar J, et al. Organizing pneumonia related to electronic cigarette use: a case report and review of literature. *Clin Respir J* 2018; 12:1295–1299
75. Kligerman S, Raptis C, Larsen B, et al. Radiologic, pathologic, clinical, and physiologic findings of electronic cigarette or vaping product use-associated lung injury (EVALI): evolving knowledge and remaining questions. *Radiology* 2020; 294:491–505
76. Blagev DP, Harris D, Dunn AC, Guidry DW, Grissom CK, Lanspa MJ. Clinical presentation, treatment, and short-term outcomes of lung injury associated with e-cigarettes or vaping: a prospective observational cohort study. *Lancet* 2019; 394:2073–2083
77. Layden JE, Ghinai I, Pray I, et al. Pulmonary illness related to e-cigarette use in Illinois and Wisconsin: final report. *N Engl J Med* 2020; 382:903–916
78. Henry TS, Kanne JP, Kligerman SJ. Imaging of vaping-associated lung disease. *N Engl J Med* 2019; 381:1486–1487
79. Henry TS, Kligerman SJ, Raptis CA, Mann H, Sechrist JW, Kanne JP. Imaging findings of vaping-associated lung injury. *AJR* 2020; 214:498–505
80. Dicpinigaitis PV, Trachuk P, Fakier F, Teka M, Suhrland MJ. Vaping-associated acute respiratory failure due to acute lipoid pneumonia. *Lung* 2020; 198:31–33
81. He T, Oks M, Esposito M, Steinberg H, Makaryus M. "Tree-in-bloom": severe acute lung injury induced by vaping cannabis oil. *Ann Am Thorac Soc* 2017; 14:468–470
82. Thota D, Latham E. Case report of electronic cigarettes possibly associated with eosinophilic pneumonitis in a previously healthy active-duty sailor. *J Emerg Med* 2014; 47:15–17
83. Thakrar PD, Boyd KP, Swanson CP, Wideburg E, Kumbhar SS. E-cigarette, or vaping, product use-associated lung injury in adolescents: a review of imaging features. *Pediatr Radiol* 2020; 50:338–344
84. Sodhi KS, Lee EY. What all physicians should know about the potential radiation risk that computed tomography poses for paediatric patients. *Acta Paediatr* 2014; 103:807–811
85. Sodhi KS, Sharma M, Lee EY, et al. Diagnostic utility of 3T lung MRI in children with interstitial lung disease: a prospective pilot study. *Acad Radiol* 2018; 25:380–386
86. Gorkem SB, Coskun A, Yikilmaz A, Zurakowski D, Mulkern RV, Lee EY. Evaluation of pediatric thoracic disorders: comparison of unenhanced fast-imaging-sequence 1.5-T MRI and contrast-enhanced MDCT. *AJR* 2013; 200:1352–1357
87. Liszewski MC, Ciet P, Lee EY. MR imaging of lungs and airways in children: past and present. *Magn Reson Imaging Clin N Am* 2019; 27:201–225